Fokker–Planck description of the scattering of radio frequency waves at the plasma edge

Kyriakos Hizanidis,[1] Abhay K. Ram,[2] Yannis Kominis,[1] and Christos Tsironis[1]

[1]*School of Electrical and Computer Engineering, National Technical University of Athens, Athens GR 15773, Greece*
[2]*Plasma Science and Fusion Center, Massachusetts Institute of Technology, Cambridge, Massachusetts 02139, USA*

In magnetic fusion devices, radio frequency (rf) waves in the electron cyclotron (EC) and lower hybrid (LH) range of frequencies are being commonly used to modify the plasma current profile. In ITER, EC waves are expected to stabilize the neoclassical tearing mode (NTM) by providing current in the island region [R. Aymar *et al.*, Nucl. Fusion **41**, 1301 (2001)]. The appearance of NTMs severely limits the plasma pressure and leads to the degradation of plasma confinement. LH waves could be used in ITER to modify the current profile closer to the edge of the plasma. These rf waves propagate from the excitation structures to the core of the plasma through an edge region, which is characterized by turbulence—in particular, density fluctuations. These fluctuations, in the form of blobs, can modify the propagation properties of the waves by refraction. In this paper, the effect on rf due to randomly distributed blobs in the edge region is studied. The waves are represented as geometric optics rays and the refractive scattering from a distribution of blobs is formulated as a Fokker–Planck equation. The scattering can have two diffusive effects—one in real space and the other in wave vector space. The scattering can modify the trajectory of rays into the plasma and it can affect the wave vector spectrum. The refraction of EC waves, for example, could make them miss the intended target region where the NTMs occur. The broadening of the wave vector spectrum could broaden the wave generated current profile. The Fokker–Planck formalism for diffusion in real space and wave vector space is used to study the effect of density blobs on EC and LH waves in an ITER type of plasma environment. For EC waves the refractive effects become important since the distance of propagation from the edge to the core in ITER is of the order of a meter. The diffusion in wave vector space is small. For LH waves the refractive effects are insignificant but the diffusion in wave vector space is important. The theoretical model is general enough to study the effect of density blobs on all propagating cold plasma waves. © *2010 American Institute of Physics*. [doi:10.1063/1.3304241]

I. INTRODUCTION

In a variety of magnetically confined plasmas, radio frequency (rf) waves in the electron cyclotron (EC) and lower hybrid (LH) range of frequencies have been, and are being, used to generate localized current. EC waves are used to modify the current profile and control the growth of the neoclassical tearing mode (NTM) instability.[1] The NTM instability leads to severe degradation of confinement and can be stabilized by driving current in the island region.[2–6] In ITER, the primary scheme for modifying the current density profile in the core in order to control NTMs will be by electron cyclotron radio frequency (ECRF) waves.[7–9] LH waves have also been used to successfully generate plasma current and modify the current profile.[10] In ITER, LH waves will not be able to access the core of the high temperature plasma but could be used to modify the current profile in the edge region and help improve the overall confinement. The EC and LH rf waves are coupled into the plasma from an external excitation structure and have to propagate through the turbulent edge region of any tokamak where the waves can get scattered.

The scattering of LH and EC waves by fluctuations has been studied in ASDEX,[11] JET,[12] and FTU.[13] The interaction of rf waves with density fluctuations in the edge region can change the characteristics of waves propagating into the core of the plasma. In ITER, the EC wave beam is expected to propagate over a large distance, of the order of the minor radius, before it interacts with electrons in the vicinity of the EC resonance. Even small changes in the properties of the launched wave at the edge could significantly influence the behavior of the wave in the core of the plasma. For example, refraction of an EC beam at the edge could modify the trajectory of the beam so that it misses its intended target— NTM islands. An understanding of the scattering of an EC beam will provide the necessary adjustments needed in the control design of the automatic alignment system steering a wave beam. In this paper, we study the modification to rf waves that can occur due to random density fluctuations in the edge region.

The density fluctuations in the edge plasma can affect the wave beam through two physically distinct mechanisms—refraction and diffraction. The former is qualitatively different from normal refraction due to changes in the refractive index as waves propagate in an inhomoge-

neous plasma—the gradual changes occurring on a scale length comparable to the minor radius. The edge is characterized by strong and intermittent turbulence dominated by convective motion of strongly nonlinear structures that are formed during the nonlinear saturation of plasma instabilities.[6] The amplitude of these fluctuations, referred to as avaloids, streamers, or blobs,[14,15] range from 5% to more than 20% of the background density. The associated scale lengths range from 10 to 30 times the local ion Larmor radius. The refractive effects on wave propagation due to these fluctuations can be quite significant if the scale length of the fluctuations is larger than the wavelength of the EC beams.[16] The diffractive effect of density fluctuations will not be considered as that analysis requires a completely different treatment.

In this paper, we study the refractive effect of fluctuations, in the form of blobs, on EC and LH waves using geometric optics analysis.[17] Along its path of propagation a rf ray will encounter a number of blobs, each one of which refracts the ray. The cumulative effect of small changes in the propagation vector of a ray due to encounters with a randomly distributed set of blobs can eventually lead to two distinctly detrimental effects. First, changes in the transverse (to the confining magnetic field) component of the wave vector can lead to an effective deflection of the ray, thereby missing the intended target region where the wave is expected to deposit its energy or momentum. Second, changes in the parallel (to the magnetic field) component of the wave vector will, in general, modify the EC resonance condition through resonance broadening, thereby affecting the spatial profile of the wave induced current.

We start our analysis with the Hamilton–Jacobi equations for geometric optics and derive, using perturbation theory, the evolution equation for wave vectors as the rays encounter density blobs. We derive a Fokker–Planck (FP) equation for the evolution of the wave vectors when the rays encounter randomly distributed blobs of varying sizes. The diffusion tensor in the FP equation is analytically derived and it describes the diffusive evolution of the ray wave vectors due to these encounters with blobs. We determine the Green's function solution by solving the spatially averaged FP equation for an initial distribution function of wave vectors that is a three-dimensional Dirac delta function. We analytically calculate the broadening of the wave vectors by taking the appropriate moments of the distribution function obtained from the FP equation. The analysis is quite general and allows for arbitrary angles of propagation of the waves with respect to the confining magnetic field. It is valid for all propagating cold plasma waves and captures the basic physics of refractive scattering of rf waves by a distribution of density blobs. In order to illustrate some results from our model, we carry out an analysis for EC and LH waves in plasma conditions similar to those that will be encountered in ITER.

This paper is divided as follows. In Sec. II we introduce the Hamilton–Jacobi ray equations and the Hamiltonian perturbation approach. We determine the general form of the diffusion tensor. In Sec. III the diffusion tensor is explicitly evaluated for simple, but general, statistical assumptions. We

FIG. 1. The coordinate system used in the model: the ζ-axis is along the group velocity of the ray, the z-axis is along the magnetic field $\mathbf{B_0}$ direction, and $\mathbf{k_0}$ is the propagation vector for the unperturbed ray.

determine the spatially averaged form of the diffusion tensor and the corresponding FP equation for rays distributed in wave vector space. In Sec. IV we solve the FP equation and determine the spreading of the propagation vectors due to the blobs. In Sec. V the consequences of scattering by blobs in the edge region are investigated for EC and LH waves in ITER-type plasma conditions. Finally, in Sec. VI the main results are summarized.

II. THE MODEL

The Hamilton–Jacobi ray equations for the independent quantities $\mathbf{k}$ and $\mathbf{r}$ are[17]

$$\frac{d\mathbf{k}}{dt} = -\nabla_{\mathbf{r}}\omega, \quad \frac{d\mathbf{r}}{dt} = \nabla_{\mathbf{k}}\omega, \quad \frac{d\omega}{dt} = \frac{\partial\omega}{\partial t}, \tag{1}$$

where $\mathbf{k}$ is the wave vector, $\omega = \omega(\mathbf{r}, \mathbf{k}, t)$ is the frequency of the rf wave, $\mathbf{r}$ is the spatial location of the ray at time t, and the nabla operators indicate the appropriate partial derivatives with respect to the subscripted variables. Equation (1) can be rewritten in terms of the refractive index $\eta = ck/\omega$ with k being the magnitude of $\mathbf{k}$. Using the identities,

$$0 = \nabla_{\mathbf{r}}k = \frac{\eta}{c}\nabla_{\mathbf{r}}\omega + \frac{\omega}{c}\nabla_{\mathbf{r}}\eta, \quad \frac{\mathbf{k}}{k} = \nabla_{\mathbf{k}}k = \frac{\eta}{c}\nabla_{\mathbf{k}}\omega + \frac{\omega}{c}\nabla_{\mathbf{k}}\eta, \tag{2}$$

the first two expressions in Eq. (1) become

$$\frac{d\mathbf{k}}{d\ell} = k\nabla_{\mathbf{r}}\left(\frac{1}{\eta}\right), \quad \frac{d\mathbf{r}}{d\ell} = \frac{\mathbf{k}}{k} + k\nabla_{\mathbf{k}}\left(\frac{1}{\eta}\right), \tag{3}$$

where $\ell = ct$. In the edge region of the plasma we will assume that the temperature is low enough so that the cold plasma approximation for the waves is valid. This is a reasonable assumption since, even with thermal effects included, the EC and LH wave dispersion relations are well presented by the cold plasma approximation. Also, the damping of waves is assumed to occur away from the plasma edge, so we can neglect temperature effects in the edge region. We will assume that the radial size of the edge region is small compared to the plasma dimensions. This allows us to neglect any spatial variation in the confining magnetic field. Then, η is a function of density alone[18]

$$\eta = \eta(\{\omega_\alpha^2(n_\alpha(\mathbf{r}))\}, \vartheta),$$

$$\omega_\alpha^2(n_\alpha(\mathbf{r})) = \frac{q_\alpha^2 n_\alpha(\mathbf{r})}{\varepsilon_0 m_\alpha}, \quad \vartheta = \cos^{-1}\left(\frac{\mathbf{k}\cdot\mathbf{i_z}}{k}\right), \tag{4}$$

where θ is the angle of propagation of the plane wave with respect to the homogeneous magnetic field, which is assumed to be along the z-direction (Fig. 1). The spatial dependence enters via the density fluctuations present in the region of propagation. Then, Eq. (3) becomes

$$\frac{d\mathbf{k}}{d\ell} = -\frac{k}{\varepsilon_0 \eta^2}\sum_\alpha \frac{q_\alpha^2}{m_\alpha}\frac{\partial\eta}{\partial\omega_\alpha^2}\nabla_{\mathbf{r}}n_\alpha(\mathbf{r}),$$

$$\frac{d\mathbf{r}}{d\ell} = \mathbf{i_k} + \frac{1}{\eta^2\sin\vartheta}\frac{d\eta}{d\vartheta}(\mathbf{i_z}\cdot\mathbf{I_T}), \tag{5}$$

where

$$\mathbf{I_T} \equiv \mathbf{I} - \mathbf{i_k}\mathbf{i_k}, \quad \mathbf{i_k} \equiv \frac{\mathbf{k}}{k}, \tag{6}$$

$\mathbf{i_k}$ is the unit vector along $\mathbf{k}$, $\mathbf{i_z}$ is the unit vector along the z-directions, $\mathbf{i_k}\mathbf{i_k}$ is a dyadic of unit vectors in $\mathbf{k}$-space, $\mathbf{I}$ is the unit dyadic, and the summation is over all species that constitute the plasma.

As the ray propagates through the plasma edge it encounters a number of blobs. We express the plasma density as a sum of a constant background density and a small fluctuating part corresponding to the blobs. The refractive index is then expanded in a Taylor series with the expansion parameter being the magnitude of the fluctuating density. Then, to first order

$$n_\alpha(\mathbf{r}) = n_{\alpha 0} + \delta n_\alpha(\mathbf{r}), \quad \eta \simeq \eta_0 + \frac{1}{\varepsilon_0}\sum_\alpha \frac{q_\alpha^2}{m_\alpha}\frac{\partial\eta_0}{\partial\omega_{\alpha 0}^2}\delta n_\alpha(\mathbf{r}). \tag{7}$$

The Hamilton–Jacobi ray equations become

$$\dot{\mathbf{k}} \equiv \frac{d\mathbf{k}}{d\ell} \simeq -\frac{k}{\varepsilon_0\eta_0^2}\sum_\alpha \frac{q_\alpha^2}{m_\alpha}\left(\frac{\partial\eta_0}{\partial\omega_{\alpha 0}^2}\right)\nabla_{\mathbf{r}}\delta n_\alpha,$$

$$\dot{\mathbf{r}} \equiv \frac{d\mathbf{r}}{d\ell} \simeq \mathbf{i_k} + \frac{1}{\eta_0^2\sin\vartheta}(\mathbf{i_z}\cdot\mathbf{I_T})$$
$$\times\left[\frac{d\eta_0}{d\vartheta} + \frac{1}{\varepsilon_0}\sum_\alpha \delta n_\alpha\frac{q_\alpha^2}{m_\alpha}\frac{d}{d\vartheta}\left(\frac{\partial\eta_0}{\partial\omega_{\alpha 0}^2}\right)\right]. \tag{8}$$

In the absence of any density blobs, these equations become

$$\frac{d\mathbf{k}}{d\ell} = 0, \quad \frac{d\mathbf{r}}{d\ell} = \mathbf{i_s}\sqrt{1 + \frac{1}{\eta_0^4}\left(\frac{d\eta_0}{d\vartheta}\right)^2}, \tag{9}$$

where

$$\mathbf{i_s} \equiv \frac{\mathbf{i_k} + \dfrac{1}{\eta_0^2\sin\vartheta}(\mathbf{i_z}\cdot\mathbf{I_T})\dfrac{d\eta_0}{d\vartheta}}{\sqrt{1 + \dfrac{1}{\eta_0^4}\left(\dfrac{d\eta_0}{d\vartheta}\right)^2}} \tag{10}$$

is the unit vector along the direction of the group velocity.

For a statistical ensemble of blobs, the correlation functions along the path of a ray are given by

$$\langle\dot{\mathbf{k}}(\mathbf{r};\mathbf{k})\dot{\mathbf{k}}(\mathbf{r}+\mathbf{i_s}\sigma;\mathbf{k})\rangle \simeq \frac{k^2}{\varepsilon_0^2\eta_0^4}\sum_{\alpha,\beta}\frac{q_\alpha^2 q_\beta^2}{m_\alpha m_\beta}\left(\frac{\partial\eta_0}{\partial\omega_{\alpha 0}^2}\right)\left(\frac{\partial\eta_0}{\partial\omega_{\beta 0}^2}\right)$$
$$\times\langle\nabla_{\mathbf{r}}\delta n_\alpha(\mathbf{r})\nabla_{\mathbf{r}}\delta n_\beta(\mathbf{r}+\mathbf{i_s}\sigma)\rangle, \tag{11}$$

$$\langle\dot{\mathbf{r}}(\mathbf{r};\mathbf{k})\dot{\mathbf{r}}(\mathbf{r}+\mathbf{i_s}\sigma;\mathbf{k})\rangle \simeq \mathbf{i_k}\mathbf{i_k} + \frac{2}{\eta_0^2\sin\vartheta}(\mathbf{i_z}\cdot\mathbf{I_T})\mathbf{i_k}\frac{d\eta_0}{d\vartheta} + \frac{1}{\eta_0^4\sin^2\vartheta}(\mathbf{i_z}\cdot\mathbf{I_T})(\mathbf{i_z}\cdot\mathbf{I_T})\left(\frac{d\eta_0}{d\vartheta}\right)^2 + \frac{1}{\eta_0^4\sin^2\vartheta}(\mathbf{i_z}\cdot\mathbf{I_T})$$
$$\times(\mathbf{i_z}\cdot\mathbf{I_T})\frac{1}{\varepsilon_0^2}\sum_{\alpha,\beta}\frac{q_\alpha^2 q_\beta^2}{m_\alpha m_\beta}\frac{d}{d\vartheta}\left(\frac{\partial\eta_0}{\partial\omega_{\alpha 0}^2}\right)\frac{d}{d\vartheta}\left(\frac{\partial\eta_0}{\partial\omega_{\beta 0}^2}\right)\langle\delta n_\alpha(\mathbf{r})\delta n_\beta(\mathbf{r}+\mathbf{i_s}\sigma)\rangle, \tag{12}$$

$$\langle \dot{\mathbf{k}}(\mathbf{r};\mathbf{k})\dot{\mathbf{r}}(\mathbf{r}+\mathbf{i}_s\sigma;\mathbf{k})\rangle$$

$$\simeq -\frac{k}{\varepsilon_0^2\eta_0^4\sin\vartheta}\sum_{\alpha,\beta}\frac{q_\alpha^2 q_\beta^2}{m_\alpha m_\beta}\left(\frac{\partial\eta_0}{\partial\omega_{\alpha 0}^2}\right)\frac{d}{d\vartheta}\left(\frac{\partial\eta_0}{\partial\omega_{\beta 0}^2}\right)$$

$$\times\langle\nabla_\mathbf{r}\delta n_\alpha(\mathbf{r})\delta n_\beta(\mathbf{r}+\mathbf{i}_s\sigma)\rangle(\mathbf{i_z}\cdot\mathbf{I_T}), \qquad (13)$$

$$\langle\dot{\mathbf{r}}(\mathbf{r};\mathbf{k})\dot{\mathbf{k}}(\mathbf{r}+\mathbf{i}_s\sigma;\mathbf{k})\rangle$$

$$\simeq -\frac{k}{\varepsilon_0^2\eta_0^4\sin\vartheta}(\mathbf{i_z}\cdot\mathbf{I_T})$$

$$\times\sum_{\alpha,\beta}\frac{q_\alpha^2 q_\beta^2}{m_\alpha m_\beta}\left(\frac{\partial\eta_0}{\partial\omega_{\alpha 0}^2}\right)\frac{d}{d\vartheta}\left(\frac{\partial\eta_0}{\partial\omega_{\beta 0}^2}\right)$$

$$\times\langle\delta n_\beta(\mathbf{r})\nabla_\mathbf{r}\delta n_\alpha(\mathbf{r}+\mathbf{i}_s\sigma)\rangle, \qquad (14)$$

where $\langle\cdots\rangle$ is an ensemble average over the distribution of blobs. On the basis of these correlations, we define a 6×6 diffusion tensor,[19]

$$\mathbf{D}(\mathbf{X})\equiv\frac{1}{\Delta s}\int_0^{\Delta s}ds\int_{-s}^{\Delta s-s}d\sigma$$

$$\times\langle\dot{\mathbf{X}}'[\mathbf{r}(s);\mathbf{k}]\dot{\mathbf{X}}'[\mathbf{r}(s)+\mathbf{i}_s\sigma;\mathbf{k}]\rangle$$

$$\simeq\int_{-\infty}^{\infty}d\sigma\langle\dot{\mathbf{X}}'[\mathbf{r}(\ell);\mathbf{k}]\dot{\mathbf{X}}'[\mathbf{r}(\ell)+\mathbf{i}_s\sigma;\mathbf{k}]\rangle, \qquad (15)$$

where $\mathbf{X}=(\mathbf{r},\mathbf{k})$ is a six-dimensional vector and Δs is an element of length along the ray over which the density fluctuations are correlated. The dot on top of $\mathbf{X}$ denotes differentiation with respect to ℓ. The main contribution to the integrand in Eq. (15) is for σ's, which are within Δs so that the approximate expression is valid. This approximation also implies that the distance over which the rays interact with blobs is smaller than Δs. The diffusion tensor describes the cumulative effect of the interaction of a ray with a randomly distributed collection of blobs. The primes refer to rates of change due to the fluctuations and are obtained from Eq. (8),

$$\dot{\mathbf{X}}'=\left[\frac{1}{\eta_0^2\varepsilon_0\sin\vartheta}(\mathbf{i_z}\cdot\mathbf{I_T})\sum_\alpha\delta n_\alpha\frac{q_\alpha^2}{m_\alpha}\frac{d}{d\vartheta}\left(\frac{\partial\eta_0}{\partial\omega_{\alpha 0}^2}\right),\right.$$

$$\left.-\frac{k}{\varepsilon_0\eta_0^2}\sum_\alpha\frac{q_\alpha^2}{m_\alpha}\left(\frac{\partial\eta_0}{\partial\omega_{\alpha 0}^2}\right)\nabla_\mathbf{r}\delta n_\alpha\right]. \qquad (16)$$

The evolution equation for a distribution of rays $f(\mathbf{X},\ell)$ is

$$\frac{\partial f}{\partial\ell}+\left[\mathbf{i_k}+\frac{1}{\eta_0^2\sin\vartheta}(\mathbf{i_z}\cdot\mathbf{I_T})\frac{d\eta_0}{d\vartheta}\right]\cdot\nabla_\mathbf{r}f$$

$$=\frac{\partial}{\partial\mathbf{X}}\cdot\left[\mathbf{D}(\mathbf{X})\cdot\frac{\partial f}{\partial\mathbf{X}}\right], \qquad (17)$$

where the differential operators on the left-hand side are along the unperturbed ray.

III. THE FP EQUATION IN k-SPACE

The spatial average of Eq. (17) over a volume V_0, occupied by the blobs, leads to

$$\frac{\partial\bar{f}}{\partial\ell}=\mathrm{div_k}(\langle\langle\mathbf{D_{kk}}(\mathbf{X})\cdot\mathrm{grad_k}f\rangle\rangle)$$

$$\simeq\mathrm{div_k}(\langle\langle\mathbf{D_{kk}}(\mathbf{X})\rangle\rangle\cdot\mathrm{grad_k}\bar{f}), \qquad (18)$$

where $\langle\langle\cdots\rangle\rangle$ denotes the spatial average. Here, we have replaced the spatially averaged inner product of the three-dimensional tensor $\mathbf{D_{kk}}$ with the $\mathbf{k}$-space gradient of the distribution function by the inner product of the spatially averaged tensor $\langle\langle\mathbf{D_{kk}}\rangle\rangle$ with the $\mathbf{k}$-space gradient of the spatially averaged distribution function,

$$\bar{f}(\mathbf{k},\ell)\equiv\langle\langle f(\mathbf{X},\ell)\rangle\rangle\equiv\frac{1}{V_0}\int dV_0 f(\mathbf{X},\ell), \qquad (19)$$

where $\mathbf{D_{kk}}$ is the submatrix of Eq. (15) associated only with the $\mathbf{k}$-space. The assumption used to obtain Eq. (18) is that the spatial scale length over the diffusion tensor varies is much longer than the spatial scale length over which the distribution function varies. This assumption follows from our initial assumption that the only source of inhomogeneity is the density fluctuations. Equation (18) is now a FP equation for the distribution function of rays distributed in the wave vector subspace.

Let us consider a Gaussian form for density fluctuations, which is independent of the plasma species,

$$\delta n_\alpha(\mathbf{r};\mathbf{r}_0)=\nu n_\alpha\exp\left(-\frac{|\mathbf{r}-\mathbf{r}_0|^2}{2(\Delta r)^2}\right), \qquad (20)$$

where ν is a dimensionless random variable, $\mathbf{r}$ is the position vector, $\mathbf{r}_0$ denotes the position of the center of the blob, and Δr is the characteristic size of a blob. From quasineutrality,

$$\sum_\alpha q_\alpha\delta n_a=\nu\exp\left(-\frac{|\mathbf{r}-\mathbf{r}_0|^2}{2(\Delta r)^2}\right)\sum_\alpha q_\alpha n_a=0. \qquad (21)$$

Equation (20) implies that the blobs are spherical and the underlying turbulence is isotropic. This is an approximation as it is known that the blobs are stretched out along the magnetic field lines due to the fast parallel particle conduction along the magnetic field.[20] However, data from the TJ-II stellarator and NSTX (Ref. 21) shows that the percentage of elongated blobs, with aspect ratio greater than 2, is less than 35%.

Let us also assume a normal probability distribution function $w(\nu)$ for the dimensionless variable ν,

$$w(\nu)=\frac{1}{\delta_0\sqrt{2\pi}}\exp\left[-\frac{(\nu-\nu_0)^2}{2\delta_0^2}\right], \qquad (22)$$

where ν_0, the mean value, and δ_0, the standard deviation, are small nominal parameters that characterize the fluctuations. Assuming that the centers $\mathbf{r_0}$ are uniformly distributed over a volume V_0, integrating over ν yields the diffusion tensor in $\mathbf{k}$-space,

$$\langle\langle \mathbf{D_{kk}} \rangle\rangle = \frac{k^2(\nu_0^2 + \delta_0^2)\sqrt{2\pi}}{4V_0(\Delta r)^3 \eta_0^6} \sum_{\alpha,\beta} \omega_{\alpha 0}^2 \omega_{\beta 0}^2 \left(\frac{\partial \eta_0^2}{\partial \omega_{\alpha 0}^2}\right)\left(\frac{\partial \eta_0^2}{\partial \omega_{\beta 0}^2}\right) \times \int_V dV_0 (\mathbf{r} - \mathbf{r_0})(\mathbf{r} - \mathbf{r_0})$$

$$\times \exp\left(-\frac{2|\mathbf{r} - \mathbf{r_0}|^2 + |(\mathbf{r} - \mathbf{r_0})\cdot \mathbf{i_s}|^2}{2(\Delta r)^2}\right). \tag{23}$$

Let $\mathbf{i_1}$ and $\mathbf{i_2}$ be two mutually orthogonal unit vectors that are perpendicular to $\mathbf{i_s}$. Then, the projection of this tensor along $\mathbf{i_1}$ and $\mathbf{i_2}$ is

$$\langle\langle \mathbf{i_1} \cdot \mathbf{D_{kk}} \cdot \mathbf{i_2} \rangle\rangle = \frac{\left[\sum_{b=x,y,z}(\mathbf{i_b}\cdot\mathbf{i_1})(\mathbf{i_b}\cdot\mathbf{i_2}) - \frac{1}{3}\sum_{b=x,y,z}(\mathbf{i_b}\cdot\mathbf{i_s})(\mathbf{i_b}\cdot\mathbf{i_1})\sum_{b=x,y,z}(\mathbf{i_b}\cdot\mathbf{i_s})(\mathbf{i_b}\cdot\mathbf{i_2})\right]}{4\sqrt{3}\,\eta_0^4 V_0}$$

$$\times \left(\frac{\pi\Delta r \omega}{c}\right)^2 (\nu_0^2 + \delta_0^2)\sum_{\alpha,\beta} \omega_{\alpha 0}^2 \omega_{\beta 0}^2 \left(\frac{\partial \eta_0^2}{\partial \omega_{\alpha 0}^2}\right)\left(\frac{\partial \eta_0^2}{\partial \omega_{\beta 0}^2}\right), \tag{24}$$

where we have used the fact that

$$(\mathbf{i_x}\cdot\mathbf{i_a})^2 + (\mathbf{i_y}\cdot\mathbf{i_a})^2 + (\mathbf{i_z}\cdot\mathbf{i_a})^2 = 1, \quad \mathbf{a} = \mathbf{1,2,s}. \tag{25}$$

If we define a Cartesian coordinate system by $(\mathbf{i_\chi}, \mathbf{i_\psi}, \mathbf{i_\zeta})$, as indicated in Fig. 1, such that $\mathbf{i_s}$ is along the ζ-direction, then the diffusion tensor in Eq. (23) is diagonalized and Eq. (18) takes on the form

$$\frac{\partial \bar{f}(\mathbf{k},\ell)}{\partial \ell} = \left[\frac{\partial}{\partial k_\zeta}\left(\langle\langle D_{\zeta\zeta}\rangle\rangle\frac{\partial}{\partial k_\zeta}\right) + \frac{\partial}{\partial k_\chi}\left(\langle\langle D_{\chi\chi}\rangle\rangle\frac{\partial}{\partial k_\chi}\right)\right.$$
$$\left. + \frac{\partial}{\partial k_\psi}\left(\langle\langle D_{\psi\psi}\rangle\rangle\frac{\partial}{\partial k_\psi}\right)\right]\bar{f}(\mathbf{k},\ell), \tag{26}$$

where

$$\begin{bmatrix} \langle\langle D_{\chi\chi}\rangle\rangle \\ \langle\langle D_{\psi\psi}\rangle\rangle \\ \langle\langle D_{\zeta\zeta}\rangle\rangle \end{bmatrix} \simeq \frac{\left(\frac{\pi\Delta r\omega}{c}\right)^2 (\nu_0^2 + \delta_0^2)\sum_{\alpha,\beta}\omega_{\alpha 0}^2\omega_{\beta 0}^2\left(\frac{\partial\eta_0^2}{\partial\omega_{\alpha 0}^2}\right)\left(\frac{\partial\eta_0^2}{\partial\omega_{\beta 0}^2}\right)}{4\sqrt{3}\,\eta_0^4 V_0}$$

$$\times \begin{bmatrix} 1 \\ 1 \\ \frac{2}{3} \end{bmatrix}. \tag{27}$$

IV. BROADENING OF THE PROPAGATION VECTOR

Let us assume that a ray is initially launched with a specific wave vector $(k_\chi, k_\psi, k_\zeta)$ in the orthogonal system shown in Fig. 1. Then,

$$\bar{f}(\mathbf{k}, \ell = 0) = \delta(k_\zeta - k_{\zeta 0})\delta(k_\chi - k_{\chi 0})\delta(k_\psi - k_{\psi 0}). \tag{28}$$

Then, the Green's function solution to Eq. (27) is

$$\bar{f}(\mathbf{k},\ell) = \frac{1}{\left(\frac{2}{3}\right)^{1/2}(4\pi D\ell)^{3/2}}$$

$$\times \exp\left[-\frac{3(k_\zeta - k_{\zeta 0})^2}{8D\ell}\right.$$

$$\left. -\frac{(k_\chi - k_{\chi 0})^2}{4D\ell} - \frac{(k_\psi - k_{\psi 0})^2}{4D\ell}\right], \tag{29}$$

where, in accordance with Eq. (27),

$$D \equiv \frac{\left(\frac{\pi\Delta r\omega}{c}\right)^2 (\nu_0^2 + \delta_0^2)\sum_{\alpha,\beta}\omega_{\alpha 0}^2\omega_{\beta 0}^2\left(\frac{\partial\eta_0^2}{\partial\omega_{\alpha 0}^2}\right)\left(\frac{\partial\eta_0^2}{\partial\omega_{\beta 0}^2}\right)}{4\sqrt{3}\,\eta_0^4 V_0} \tag{30}$$

is the scalar diffusion coefficient. The derivatives in Eq. (30) are given in the Appendix.

Since $\mathbf{k_0}$, $\mathbf{i_s}$, and the magnetic field are all in the same plane, the Jacobian of a transformation to any other orthogonal coordinate system, obtained by rotation around the x-axis, is unity. In a frame in which the magnetic field is along the z-axis, Eq. (29) becomes

$$\bar{f}(\Delta\mathbf{k},\ell) = \frac{1}{\left(\frac{2}{3}\right)^{1/2}(4\pi D\ell)^{3/2}}\exp\left[-\frac{|\Delta\mathbf{k}|^2}{4D\ell} - \frac{(\Delta\mathbf{k}\cdot\mathbf{i_s})^2}{8D\ell}\right], \tag{31}$$

where $\Delta\mathbf{k} = \mathbf{k} - \mathbf{k_0}$. The scattering of the ray by density blobs broadens the propagation vector so that it acquires components perpendicular to the $(z\text{-}y)$ plane (Fig. 1).

Let φ_B be the azimuthal angle with respect to the magnetic field such that

$$\Delta k_x = \Delta k_\perp \cos\varphi_B, \quad \Delta k_y = \Delta k_\perp \sin\varphi_B \tag{32}$$

with

$$\Delta k_\parallel \equiv \Delta k_z, \quad \Delta k_\perp \equiv \sqrt{(\Delta k_x)^2 + (\Delta k_y)^2}. \tag{33}$$

In this cylindrical coordinate system,

$$\hat{f}(\Delta k_\parallel, \Delta k_\perp, \varphi_B, \ell) = \frac{(\Delta k_\perp)\exp\left[-\dfrac{(\Delta k_\perp)^2(2 + \sin^2\alpha \sin^2\varphi_B) + (\Delta k_\parallel)^2(2 + \cos^2\alpha) + \Delta k_\perp \Delta k_\parallel \sin 2\alpha \sin\varphi_B}{8D\ell}\right]}{\left(\frac{2}{3}\right)^{1/2}(4\pi D\ell)^{3/2}}, \tag{34}$$

where α is the angle between the group velocity and the z-axis. From Eqs. (4) and (9),

$$\alpha = \cos^{-1}\left[\frac{\eta_0^2 \cos\vartheta + \dfrac{d\eta_0}{d\vartheta}\sin\vartheta}{\sqrt{\eta_0^4 + \left(\dfrac{d\eta_0}{d\vartheta}\right)^2}}\right] \tag{35}$$

with $d\eta_0/d\theta$ given in the Appendix. By taking moments of the distribution function in Eq. (34) along a ray path of distance L_0 along which blobs exist, we obtain the rms values of $\Delta\mathbf{k}$,

$$\begin{bmatrix} \Delta k_x^{\mathrm{rms}} \\ \Delta k_y^{\mathrm{rms}} \\ \Delta k_\parallel^{\mathrm{rms}} \end{bmatrix} = \left[\frac{1}{L_0}\int_0^{L_0} d\ell \int_{-\infty}^{\infty} d\Delta k_\parallel \int_0^{\infty} d\Delta k_\perp \int_0^{2\pi} d\varphi_B\right.$$
$$\left.\times \begin{bmatrix} (\Delta k_x)^2 \\ (\Delta k_y)^2 \\ (\Delta k_z)^2 \end{bmatrix} \hat{f}(\Delta k_\parallel, \Delta k_\perp, \varphi_B, \ell)\right]^{1/2}$$
$$= \frac{2\sqrt{6}}{9}\sqrt{L_0 D}\begin{bmatrix} \sqrt{3} \\ \sqrt{3 - \sin^2\alpha} \\ \sqrt{3 - \cos^2\alpha} \end{bmatrix}. \tag{36}$$

The magnitude of the rms values of the three components are not equal so that the broadening of the wave vector does not possess spherical symmetry. From Eq. (36), we obtain

$$\Delta k_\perp^{\mathrm{rms}} = \sqrt{(\Delta k_x^{\mathrm{rms}})^2 + (\Delta k_y^{\mathrm{rms}})^2} = \frac{2\sqrt{6}}{9}\sqrt{L_0 D}\sqrt{6 - \sin^2\alpha}. \tag{37}$$

Thus, the spreading of the wave vector component transverse to the magnetic field is a maximum when $\alpha = 0$, i.e., when the ray is propagating along the magnetic field. The spreading of the wave vector component parallel to the magnetic field is a maximum for $\alpha = \pi/2$, i.e., when the ray is propagating perpendicular to the magnetic field. Furthermore, the locus of $\Delta\mathbf{k}$ is the surface of an oblate ellipsoid with its center at the tip of the propagation vector $\mathbf{k}$ and its axis along the z-axis. The rms broadening of the wave vector in the $(y$-$z)$ plane,

$$\Delta k_{(y,z)}^{\mathrm{rms}} = \sqrt{(\Delta k_y^{\mathrm{rms}})^2 + (\Delta k_z^{\mathrm{rms}})^2} = \frac{2\sqrt{30}}{9}\sqrt{L_0 D} \tag{38}$$

is independent of α. From Eq. (30), the broadening in the transverse and parallel directions is

$$\begin{bmatrix} \dfrac{\Delta k_\perp^{\mathrm{rms}}}{k} \\ \dfrac{\Delta k_\parallel^{\mathrm{rms}}}{k} \end{bmatrix} = \frac{3^{1/4}(2\pi)^{1/2}}{9}\frac{\sqrt{\Sigma_{\alpha,\beta}\omega_{\alpha 0}^2 \omega_{\beta 0}^2\left(\dfrac{\partial\eta_0^2}{\partial\omega_{\alpha 0}^2}\right)\left(\dfrac{\partial\eta_0^2}{\partial\omega_{\beta 0}^2}\right)}}{\eta_0^3}$$
$$\times \begin{bmatrix} \sqrt{6 - \sin^2\alpha} \\ \sqrt{3 - \cos^2\alpha} \end{bmatrix}b_0, \tag{39}$$

where

$$b_0 \equiv \sqrt{g_0(\nu_0^2 + \delta_0^2)}, \quad g_0 \equiv \frac{\pi\Delta r^2 L_0}{V_0}. \tag{40}$$

The parameter $g_0 < 1$ is a measure of the number of blobs encountered by a ray in a volume V_0.

The effect of the transverse broadening of the wave vector leads to an effective angular deflection of the ray by a small angle $\Delta\alpha$ with respect to the path of the unperturbed ray. From Eq. (35),

$$|\Delta\alpha| = \left|1 + \eta_0 \frac{\eta_0 \dfrac{\partial^2\eta_0}{\partial\vartheta^2} - 2\left(\dfrac{\partial\eta_0}{\partial\vartheta}\right)^2}{\eta_0^4 + \left(\dfrac{\partial\eta_0}{\partial\vartheta}\right)^2}\right||\Delta\vartheta|, \tag{41}$$

where

$$\Delta\vartheta = \sin^{-1}\left(\frac{\Delta k_\perp^{\mathrm{rms}}}{k}\right) \tag{42}$$

is of the same order as g.

Let us consider the principal cold plasma modes propagating across the magnetic field, i.e., $\theta = \pi/2$. Using the Stix notation[18] (see the Appendix) for the extraordinary X mode with $\eta^2 = RL/S$,

$$\left|\frac{\Delta\alpha}{\Delta\vartheta}\right|_X = \left|1 - \frac{D^2 P}{16S(RL - PS)}\left(\frac{S}{RL}\right)^{1/2}\right|, \tag{43}$$

where $S = (R + L)/2$ and $D = (R - L)/2$. For the ordinary O mode with $\eta^2 = P$, we obtain

$$\left|\frac{\Delta\alpha}{\Delta\vartheta}\right|_O = \left|1 - \frac{(P - R)(P - L)}{\sqrt{P}(RL - PS)}\right|. \tag{44}$$

Let us next consider the principal cold plasma modes propagating along the magnetic field, i.e., $\theta = 0$. For the right-hand circularly polarized mode given by $\eta^2 = R$, we obtain

$$\left| \frac{\Delta \alpha}{\Delta \vartheta} \right|_R = \left| 1 - \frac{P - R}{P\sqrt{R}} \right|, \tag{45}$$

while for the left-hand circularly polarized mode given by $\eta^2 = L$, we get

$$\left| \frac{\Delta \alpha}{\Delta \vartheta} \right|_L = \left| 1 - \frac{P - L}{P\sqrt{L}} \right|. \tag{46}$$

The broadening of the wave vector along the direction of the magnetic field results in a broadening of the parallel refractive index,

$$\Delta \eta_\parallel^{\text{rms}} = \frac{c \Delta k_\parallel^{\text{rms}}}{\omega} = \eta \frac{\Delta k_\parallel^{\text{rms}}}{k}. \tag{47}$$

Any cold plasma wave, propagating at an arbitrary angle to the magnetic field, is described by a linear combination of the principal modes. The effect of scattering by density blobs can be determined for any frequency wave using the above formalism.

V. NUMERICAL RESULTS

The analytical results from the model developed above are used to illustrate the diffusive effect of blob scattering on rf waves in ITER-type plasmas. For an electron-deuterium plasma, we assume an edge magnetic field of 4.13 T, an edge electron density of $n_e = 10^{19}$ m^{-3}, and a wave frequency of 170 GHz for EC waves. The wave frequency is resonant at a magnetic field of 5.51 T in the core when the relativistic shift due to 10 keV electrons is included. From the present experiments, the relative amplitude of edge fluctuations is within the range of $\nu_0 \approx 10\% - 50\%$.[20] We will assume that in ITER $\nu_0 = \delta_0 = 0.2$, i.e., the relative density increment is 20%. For an edge plasma temperature of 200 eV,[22] the ion Larmor radius is about 0.5 mm. Experimental evidence[20] suggests that the fluctuation spectrum peaks around $\Delta r/\rho_s \approx 15 - 30$, so that, at the edge, Δr can be as large as 1.5 cm. The number of blobs along the poloidal direction in a flux surface is $N_b = L_p/(2\Delta r)$, where L_p is the poloidal arc length. In the radial direction, the number of blobs is $N_r = \Delta_b/(2\Delta r)$, where Δ_b is a measure of the radial distance traveled by the blobs. Estimates based on the experimental data from DIII-D and Alcator C-Mod (Ref. 14) suggest that Δ_b is between 3 and 15 cm. Thus, in a poloidal plane, there are roughly $N_p = N_b \times N_r$ blobs with a total occupied volume of $V_0 = 4\pi(\Delta r)^3 N_p/3 = \pi \Delta r L_p \Delta_b/3$. Assuming $L_0 \approx 0.2 - 0.3$ m and $L_p \approx 0.6$ m, the ray-blob encounter ratio $g_0 = \pi(\Delta r)^2 L_0/V_0 = 3\Delta r L_0/(L_p \Delta_b)$ is between 0.15 and 0.7. We will assume that $g_0 = 0.6$. From Eq. (40) it is evident that both the ray deflection and the broadening of the parallel refractive index scale in proportion to the blob size and the relative density increment in the blob.

In Fig. 2 we display results for the O mode (top row) and the X mode (bottom row) for parameters indicated above. In the first column the refractive index is plotted as a function
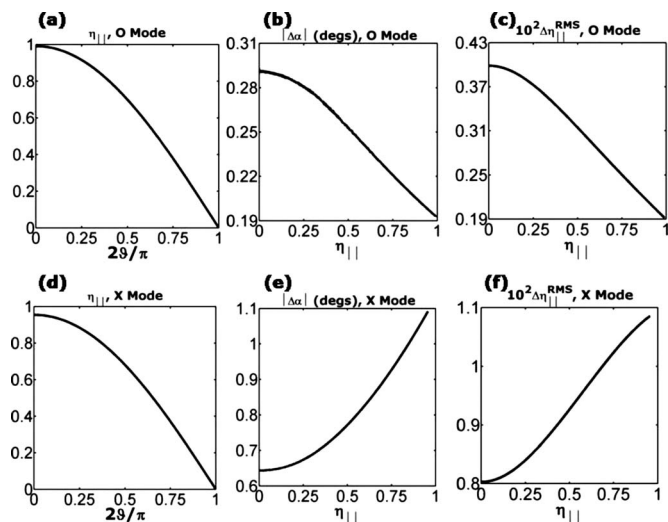

FIG. 2. Plots (a)–(c) are for the X mode and (d)–(f) are for the O mode. (a) and (d) are plots of the parallel refractive index as a function of the propagation angle θ. (b) and (e) are plots for the angle of deflection, while (c) and (f) are for the broadening of the parallel refractive index plotted as function of the parallel refractive index. The electron density at the edge is 10^{-19} m^{-3}, the wave frequency is 170 GHz, and $g_0 = 0.6$.

of θ. In the second column, we plot the rms angular deflection of the ray in the (y-z) plane as a function of the parallel refractive index $\eta_\parallel$. In the third column we plot the rms broadening of $\eta_\parallel$ as a function of $\eta_\parallel$. It is evident that the fluctuations affect the X mode more than the O mode. The X mode undergoes three times as much ray deflections and broadening as the O mode. For the O mode the maximum deflection and broadening occur at $\eta_\parallel = 0$ ($|\Delta\alpha| \approx 0.3°$, $\Delta\eta_\parallel^{\text{rms}} \approx 40\%$), while for the X mode the maximum occurs at $\eta_\parallel = 1$ ($|\Delta\alpha| \approx 1.1°$, $\Delta\eta_\parallel^{\text{rms}} \approx 110\%$). If we assume that 20%–30% of the radial propagation distance in the ITER plasma is populated by blobs, then these results imply that an O mode beam will be deflected by about 5 mm, while an X mode beam will be deflected by about 2 cm/m of ray propagation. Since the effect on the parallel refractive index for each wave is small, the main effect of the blobs is to deflect the EC beams.

In toroidal plasmas the launched ECRF waves are a linear combination of modes propagating across the magnetic field and those propagating along the magnetic field. We are better able to illustrate the ray deflection and the broadening of the parallel refractive index by looking at the principal modes propagating strictly across or along the magnetic field. In Fig. 3 the behavior of the rays for the associated four fundamental modes is illustrated. In the figures, the light gray shaded area corresponds to a region where both $\Delta k_\perp^{\text{rms}}/k$ and $\Delta k_\parallel^{\text{rms}}/k$ are greater than 0.1—this is just to illustrate that our results are within the approximations we have made in our analytical model. In Figs. 3(a) and 3(b) we plot, for the L mode propagating along the magnetic field, the deflection of the ray and the broadening of the parallel refractive index, respectively, as a function of the normalized edge ion density n_i/n_{i0}, where $n_{i0} = 10^{19}$ m^{-3}. In Figs. 3(c) and 3(d) we plot the same for the R mode. In Figs. 3(e) and 3(f) we plot the deflection and broadening, respectively, for the O mode
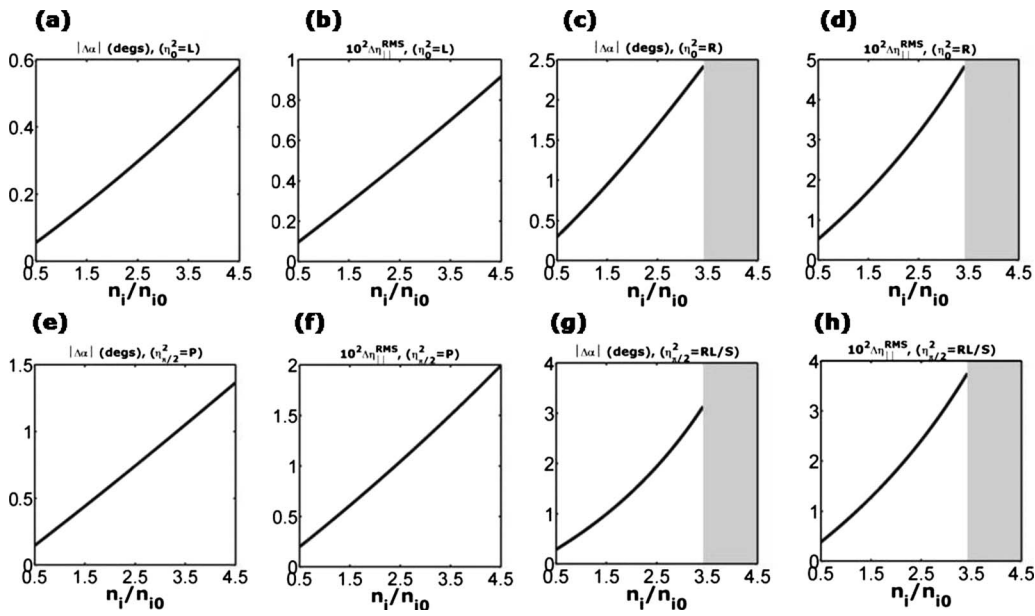
FIG. 3. (a) and (b) are plots of the ray deflection angle (in degrees) and the broadening in the parallel refractive index, respectively, as a function of the normalized edge ion density n_i/n_{i0} ($n_{i0}=10^{19}$ m^{-3} is the reference deuterium ion density) for the L mode propagating along $\mathbf{B_0}$. (c) and (d) are the corresponding plots for the R mode. (e) and (f) are the corresponding plots for the O mode across $\mathbf{B_0}$, while (g) and (h) are for the X mode. In the shaded regions $\Delta k_{\perp}^{\mathrm{rms}}/k$ and $\Delta k_{\parallel}^{\mathrm{rms}}/k$ are greater than 0.1.

propagating across the magnetic field. Figures 3(g) and 3(h) are for the X mode. We note that the X mode is more affected by the scattering process than the other EC modes. It undergoes a larger ray deflection than other modes and the broadening of its parallel refractive index is comparable to the other modes. These effects increase as the density at the edge increases. The deflection for all modes ranges from 1° to 4° for edge densities ranging from 1.5×10^{19} to 3×10^{19} m^{-3}. These angles correspond to a deflection of the ray between 1.5 and 7 cm/m of propagation. For the transverse modes, the deflection of the ray is marginally beyond the average dimensions of an NTM island. The associated broadening of the parallel refractive index is rather small and limited to a few percent.

In Fig. 4 the effect of fluctuations for all the modes is illustrated. In Figs. 4(a) and 4(b) we plot contours for the angular deflection of the O and X modes, respectively, as a function of $\eta_{\parallel}$ and n_i/n_{i0}. Figures 4(c) and 4(d) are the contour plots for the associated broadening of $\eta_{\parallel}$ for the O and X modes, respectively. The small shaded areas at the right edge of Fig. 4(b) and 4(d) are where $\Delta k_{\perp}^{\mathrm{rms}}/k$ and $\Delta k_{\parallel}^{\mathrm{rms}}/k$ are greater than 0.15. The effect of density fluctuations is, in general, more pronounced for the X modes than that in the O modes. The ray deflections are significant for the entire range of $\eta_{\parallel}$, while the associated broadening of $\eta_{\parallel}$ is rather small.

In Figs. 5 we plot the results for the slow LH waves. Figures 5(a)–5(c) are for $\eta_{\parallel}$, the deflection angle, and the broadening of $\eta_{\parallel}$, respectively, as a function of θ. We primarily consider results in the vicinity of $\theta=\pi/2$, i.e., nearly perpendicular propagation. The horizontal axis is the ratio $\omega/\omega_{\mathrm{LH}}$ of the wave frequency to the LH frequency in the plasma core where the ion plasma density is 10^{20} m^{-3} and the magnetic field is 5.51 T ($f_{\mathrm{LH}}\approx1.28$ GHz). Usually in experiments the wave frequency is chosen somewhere in the

range of $3\omega_{\mathrm{LH}}$ to $4\omega_{\mathrm{LH}}$. The dark gray area corresponds to the evanescent region of the wave, while in the light gray region, adjacent to the evanescent region, $\Delta k_{\perp}^{\mathrm{rms}}/k$ and $\Delta k_{\parallel}^{\mathrm{rms}}/k$ are greater than 0.015. The density fluctuations can
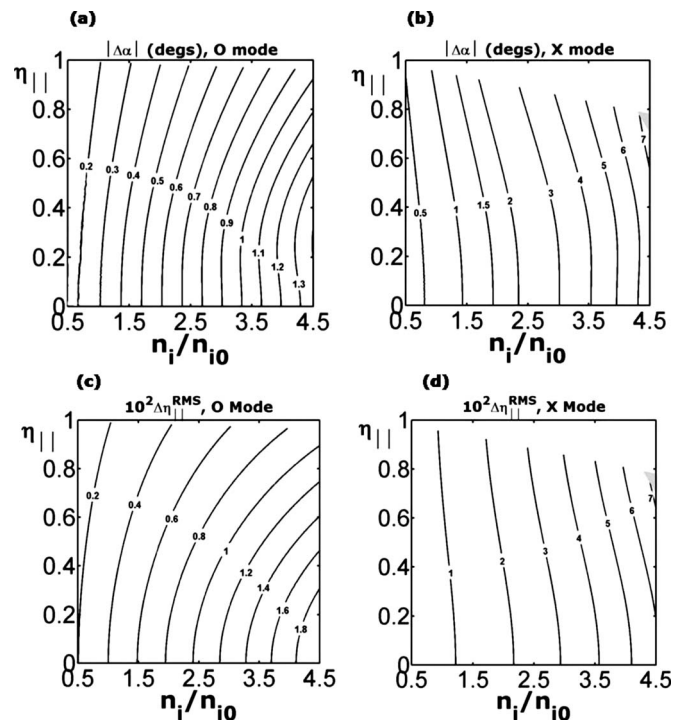

FIG. 4. (a) and (b) are contour plots for the angular deflection (in degrees) as a function of the parallel refractive index and n_i/n_{i0} for the O and X modes, respectively. (c) and (d) are contour plots of the associated broadening of the parallel refractive index for the O and X modes, respectively. In the shaded regions on the right edges of (b) and (d) $\Delta k_{\perp}^{\mathrm{rms}}/k$ and $\Delta k_{\parallel}^{\mathrm{rms}}/k$ are greater than 0.15. The wave frequency is 170 GHz and $g_0=0.6$.
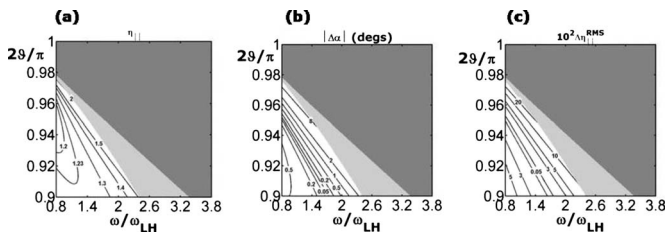
FIG. 5. (a), (b), and (c) are contour plots of the parallel refractive index, the deflection angle (in degrees, and the broadening of the parallel refractive index, respectively, as functions of $\theta \approx \pi/2$ and ω/ω_{LH}. ω_{LH} is the LH frequency in the core of the plasma, where the deuterium density is $n_i = 10^{20}$ m^{-3} and the magnetic field is 5.51 T. In the dark gray region the LH wave is evanescent, while in the light gray regions $\Delta k_\perp^{rms}/k$ and $\Delta k_\parallel^{rms}/k$ are greater than 0.015. The density at the edge is 10^{-19} m^{-3} and $g_0 = 0.6$.
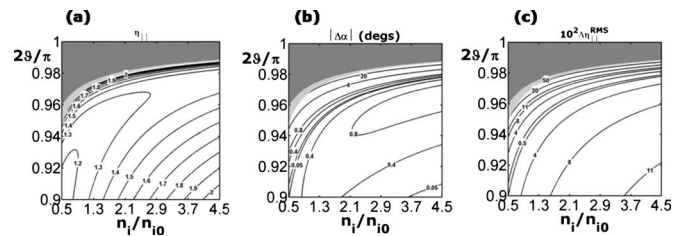

FIG. 6. (a), (b), and (c) are contour plots of the parallel refractive index, the deflection angle (in degrees), and the broadening of the parallel refractive index, respectively, as functions of $\theta \approx \pi/2$ and n_i/n_{i0}. The parameters are the same as in Fig. 5.

lead to deflections of as large as 8°–10°. The associated broadening of the parallel refractive index is more than 20%, which is significantly larger than for the EC waves. As the edge plasma density increases, the effect of fluctuations becomes very significant. In Figs. 6(a)–6(c) contour plots of $\eta_\parallel$, the deflection angle, and the broadening of $\eta_\parallel$, respectively, are plotted as functions of θ and n_i/n_{i0}. Again, the dark gray area corresponds to the evanescent region of the wave, while in the light gray regions both $\Delta k_\perp^{rms}/k$ and $\Delta k_\parallel^{rms}/k$ are greater than 0.015. For $\eta_\parallel = 2$ and an edge density of $n_i = 2 \times 10^{19}$ m^{-3}, the deflection can be as large as 20°, while the broadening of the parallel refractive index can be as large as 50%. For such a large broadening of the parallel refractive index, the LH waves will lead to a broader current profile—the larger parallel wave numbers damping closer to the edge of the plasma, while the smaller wave numbers propagating farther into the plasma away from the edge region.

VI. CONCLUSIONS

We have derived a FP diffusion equation for the scattering of rays by density fluctuations in the form of blobs. We have assumed spherical blobs, distributed randomly, in the edge region of a tokamak plasma. The propagation of the rays is given by geometric optics equations for a cold plasma. In the edge region of the plasma where the fluctuations persist, we assume that the temperature is low and that the waves are not damped. Then, the propagation of EC and LH waves is well approximated by the cold plasma model. We can then evaluate the diffusion coefficients analytically and the resulting FP equation is solved in the absence of magnetic shear and background density gradients. These effects are not amenable to analytical manipulations. However, they can be included in a straightforward fashion in a numerical code. The assumption that the blobs are spherical is for analytical tractability, which can also be generalized in numerical simulations. The model presented in this paper is capable of revealing the basic scaling laws and dependencies of the deflection of a wave beam as a function of the angle of propagation, the frequency of the wave, the amplitude of the density fluctuations, and the density of the blobs.

We have shown that the effect of edge turbulence on the propagation of rf waves in the EC range of frequencies can be sizable. For a perpendicularly propagating X mode both,

the deflection of the ray and the broadening of the parallel wave spectrum can be quite significant. For the O mode the effects due to turbulence are less severe. In ITER the EC beam will propagate at an angle to the magnetic field so that the wave is a linear combination of the X and O modes propagating normal to the magnetic field. Thus, the deflection could be large enough that the beam is deflected away from a NTM island. From our numerical results, we find that the deflection can be between 2 and 7 cm when the EC rays reach the core of an ITER plasma. The deflection increases as the density in the blobs increases. Associated with the deflection of a EC ray is a broadening of the parallel wave number. This broadening can be a few percent of the initial wave number of the ray near the edge of the plasma. The broadening of the parallel wave number spectrum can reduce the efficiency of current drive by EC waves. The larger parallel wave numbers damp farther away from a NTM island than the smaller ones. The broadening of the parallel spectrum of the waves increases as the blob density increases.

Finally, for the case of rf waves in the LH range of frequencies, the effect of density fluctuations can be quite important. While the ray deflection for ITER-type parameters is around 20°, it is important to note that the LH waves, in contrast to EC waves, will damp nearer the edge of the plasma. The deflection of the LH ray will strongly modify the spatial structure of the region where the LH waves deposit their momentum and drive plasma current. The broadening of the wave numbers can be as large as 50%. This broadening will, in turn, broaden the current profile and affect the current drive efficiency.

APPENDIX: COLD PLASMA REFRACTIVE INDEX

The Åström and Allis[18] expression for the angle of propagation of a wave is

$$\tan^2 \vartheta = \frac{P(\eta_0^2 - L)(\eta_0^2 - R)}{(LR - S\eta_0^2)(\eta_0^2 - P)}, \tag{A1}$$

where θ is the angle between **k** and the magnetic field,

$$P = 1 - \sum_\alpha \frac{\omega_{p\alpha}^2}{\omega^2}, \quad R = 1 - \sum_\alpha \frac{\omega_{p\alpha}^2}{\omega(\omega + \omega_{c\alpha})},$$

$$L = 1 - \sum_\alpha \frac{\omega_{p\alpha}^2}{\omega(\omega - \omega_{c\alpha})}, \tag{A2}$$

$\omega_{p\alpha}$ and $\omega_{c\alpha}$ are the plasma frequency and the cyclotron frequency, respectively, for the species α, and $S = (R+L)/2$. Upon differentiating with respect $\omega_{p\alpha}^2$, we obtain

$$\frac{\partial \eta_0^2}{\partial \omega_\alpha^2} = \frac{\eta_0^2}{2P\{\eta_0^4(2S^2 - PS - LR) + LR[2\eta_0^2(P-S) + LR - PS]\}}\{2\eta_0^6(PS' - P'S) + 2\eta_0^4[(LR + 2S^2)P' - P(LR)' - P^2 S']$$
$$+ 2\eta_0^2[P^2(LR)' - 3P'SLR] + P(\eta_0^2 - P)(L'R^2 + L^2 R') + 2L^2 R^2 P'\}, \tag{A3}$$

where prime denotes differentiation with respect to $\omega_{p\alpha}^2$. Differentiating Eq. (A1) with respect to θ, we get

$$\frac{d\eta_0^2}{d\vartheta} = \frac{2\eta_0^2(\eta_0^2 - L)(\eta_0^2 - R)[\eta_0^2(P-S) + LR - PS]}{[\eta_0^4(PS - 2S^2 + LR) - 2\eta_0^2(P-S)LR + PSLR - L^2 R^2]\tan(\vartheta)}. \tag{A4}$$

This expression can be differentiated once more with respect to θ to provide the second derivative in Eq. (41).

[1]R. Aymar, V. A. Chuyanov, M. Huguet, Y. Shimomura, ITER Joint Central Team, and ITER Home Teams, Nucl. Fusion **41**, 1301 (2001).
[2]H. Zohm, G. Gantenbein, G. Giruzzi, S. Günter, F. Leuterer, M. Maraschek, J. Meskat, A. G. Peeters, W. Suttrop, D. Wagner, M. Zabiégo, ASDEX Upgrade Team, and ECRH Group, Nucl. Fusion **39**, 577 (1999).
[3]G. Giruzzi, M. Zabiégo, T. A. Gianakon, X. Garbet, A. Cardinali, and S. Bernabei, Nucl. Fusion **39**, 107 (1999).
[4]Q. Yu, S. Gunter, G. Giruzzi, K. Lackner, and M. Zabiego, Phys. Plasmas **7**, 312 (2000).
[5]M. Maraschek, G. Gantenbein, Q. Yu, H. Zohm, S. Günter, F. Leuterer, A. Manini, ECRH Group, and ASDEX Upgrade Team, Phys. Rev. Lett. **98**, 025005 (2007).
[6]A. Isayama, Y. Kamada, S. Ide, K. Hamamatsu, T. Oikawa, T. Suzuki, Y. Neyatani, T. Ozeki, Y. Ikeda, K. Kajiwara, and JT-60 Team, Plasma Phys. Controlled Fusion **42**, L37 (2000).
[7]M. A. Henderson, S. Albert, P. Benin, T. Bonicelli, R. Chavan, D. Campbell, S. Cirant, G. Dammertz, O. Dormicchi, O. Dumbrajs, D. Fasel, T. P. Goodman, R. Heidinger, J.-P. Hogge, W. Kasparek, C. Lievin, B. Piosczyk, E. Poli, G. Ramponi, G. Saibene, O. Sauter, A. Serikov, G. Taddia, M. Thumm, M. Q. Tran, A. G. A. Verhoevenk, and H. Zohm, Fusion Eng. Des. **82**, 454 (2007).
[8]H. Zohm, G. Gantenbein, A. Gude, S. Günter, F. Leuterer, M. Maraschek, J. P. Meskat, W. Suttrop, Q. Yu, ASDEX Upgrade Team, and ECRH Group (AUG), Nucl. Fusion **41**, 197 2001).
[9]R. J. La Haye, Phys. Plasmas **13**, 055501 (2006).
[10]G. T. Hoang, A. Bécoulet, J. Jacquinot, J.F. Artaud, Y. S. Bae, B. Beaumont, J. H. Belo, G. Berger-By, J. P. S. Bizarro, P. Bonoli, M.H. Cho, J. Decker, L. Delpech, A. Ekedahl, J. Garcia, G. Giruzzi, M. Goniche, C. Gormezano, D. Guilhem, J. Hillairet, F. Imbeaux, F. Kazarian, C. Kessel, S. H. Kim, J. G. Kwak, J. H. Jeong, J. B. Lister, X. Litaudon, R. Magne, S. Milora, F. Mirizzi, W. Namkung, J. M. Noterdaeme, S. I. Park, R. Parker, Y. Peysson, D. Rasmussen, P. K. Sharma, M. Schneider, E. Synakowski, A. Tanga, A. Tuccillo, and Y. X. Wan, Nucl. Fusion **49**, 075001 (2009).
[11]V. Pericoli-Ridolfini, L. Giannone, and R. Bartiromo, Nucl. Fusion **34**, 469 (1994).
[12]K. M. Rantamaeki, A. N. Saveliev, T. J. J. Tala, J. A. Heikkinen, P. I. Strand, J. Weiland, G. Corrigan, and JET EFDA Contributors, Proceedings of the 32nd EPS Conference, 2005, Vol. 41, p. 197.
[13]G. Calabro, V. P. Ridolfini, L. Panaccione, and FTU Team, Europhysics Conference Abstract, 2006, Vol. 30I, p. 5.077.
[14]S. I. Krasheninnikov, Phys. Lett. A **370**, 283368 (2001).
[15]S. Benkadda, T. Dudok de Wit, A. Verga, A. Sen, ASDEX Team, and X. Garbet, Phys. Rev. Lett. **73**, 3403 (1994).
[16]T. A. Carter, Phys. Plasmas **13**, 010701 (2006).
[17]I. B. Bernstein, Phys. Fluids **18**, 320 (1975).
[18]T. H. Stix, *Waves in Plasmas* (Springer-Verlag, New York, 1992).
[19]S. Chandrasekhar, Rev. Mod. Phys. **15**, 1 (1943).
[20]G. D. Conway, Plasma Phys. Controlled Fusion **50**, 124026 (2008).
[21]J. A. Alonso, S. J. Zweben, P. Carvalho, J. L. de Pablos, E. de la Cal, C. Hidalgo, T. Klinger, B. Ph. van Milligen, R. J. Maqueda, M. A. Pedrosa, C. Silva, M. Spolaore, H. Thomsen, and TJ-II team, Plasma Phys. Controlled Fusion **48**, B465 (2006).
[22]K. McCormick, N. Asakura, S. Bosch, S. Davies, S. Fielding, K. Itami, H. Kawashima, B. LaBombard, B. Lipschultz, A. Loarte, R. Monk, G. Porter, J. Schweinzer, M. Shimada, and M. Sugihara, J. Nucl. Mater. **266–269**, 99 (1999).